Increasing pumping efficiency in a micro throttle pump by enhancing displacement amplification in an elastomeric substrate

T Fujiwara[1], I D Johnston[2], M C Tracey[2] and C K L Tan[2]

[1] Department of Mechanical Engineering, Faculty of Engineering, Tokyo City University, 1–28–1 Tamazutsumi, Setagya-ku, Tokyo 158–8557, Japan
[2] Science and Technology Research Institute, University of Hertfordshire, College Lane, Hatfield, Hertfordshire AL10 9AB, UK

E-mail: `tfujiwa@tcu.ac.jp`

Abstract. Fluid transport is accomplished in a micro throttle pump (MTP) by alternating deformation of a micro channel cast into a PDMS elastomeric substrate. The active deformation is achieved using a bimorph PZT piezoelectric disk actuator bonded to a glass diaphragm. The bimorph PZT deflects the diaphragm as well as alternately pushing and pulling the elastomer layer providing displacement amplification in the PDMS directly surrounding the micro channel. In order to improve pumping rates we have embedded a PMMA ring into the PMDS substrate which increases the magnitude of the displacement amplification achieved. FEM simulation of the elastomeric substrate deformation predicts that the inclusion of the PMMA ring should increase the channel deformation. We experimentally demonstrate that inclusion of a PMMA ring, having a diameter equal to that of the circular node of the PZT/glass/PDMS composite, increase in the throttle resistance ratio by 40 % and the maximum pumping rate by 90 % compared to an MTP with no ring.

Submitted to: *J. Micromech. Microeng.*

Nomencliature

$$
\begin{array}{rcl}
f & : & \text{pump drive frequency} \\
h & : & \text{channel height } (z_t - z_b) \\
P & : & \text{back pressure} \\
Q & : & \text{flow rate} \\
R & : & \text{flow resistance } (P/Q) \\
R_{close} & : & \text{flow resistance when the throttle closes} \\
R_{close}/R_{open} & : & \text{throttle resistance ratio} \\
R_{open} & : & \text{flow resistance when the throttle opens} \\
x & : & \text{main flow direction} \\
y & : & \text{span direction} \\
z & : & \text{height direction} \\
z_b & : & \text{height of the channel bottom} \\
z_t & : & \text{height of the channel top} \\
\Delta h & : & \text{increment of the channel height } h \text{ when the device is deformed}
\end{array}
$$

1. Introduction

Pumping elements are essential for many microfluidic devices, micro electro mechanical systems (MEMS) and micro total analysis systems (μ-TAS). Over recent years many different types of micropump have been developed to achieve fluid transport within these microenvironments [1, 2] and the broad adoption of elastomer based microfluidic device fabrication has resulted in a wealth of cheap and easy to manufacture passive flow structures [3].

As has been previously reported [4], elastomeric substrates allow substrate material to substantially impinge below the footprint of an actuator, provided that other design constraints are considered. This means that in an elastomeric substrate it is not necessary for a pump chamber to match either the size or shape of the piezoelectric actuator. Utilising this feature, a new mechanism of microfluidic pumping only possible using elastic substrates was reported by Johnston et al [4, 5, 6, 7]. In place of conventional fully closing valves this pumping technique exploits 'throttling': the use of variable cross-section flow-constrictions to regulate fluid flow, to control the flow of fluid.

The fact that microthrottles do not fully close, allied to their construction from elastic materials, makes them highly suited to the pumping of solid phase inclusions such as polystyrene microbeads, as has been previously reported [6]. The non-closing action means they are not restricted by the 'stiction' effects of fully closing elastomeric surfaces, allowing higher frequency operation which may well be suited to micromixing applications [8, 9, 10].

In this study we are concerned with the linear micro throttle pump (LMTP) which is a single PZT design employing a simple double depth micro fluidic structure incorporating an atypical rectangular pumping channel with two micro throttles to
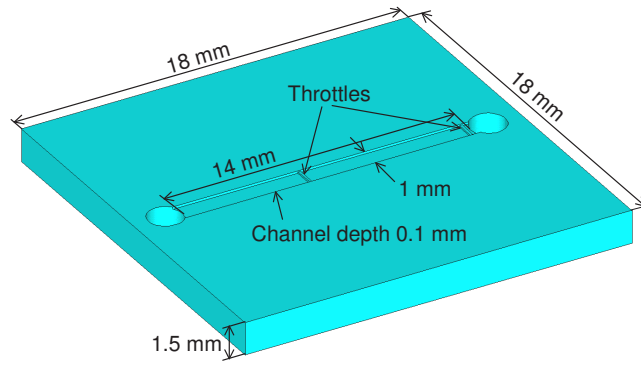
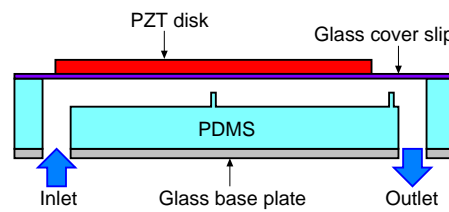**Figure 1.** Geometry of the micro channel cast on a PDMS substrate.

Figure 2. Basic components of the micro throttle pump.
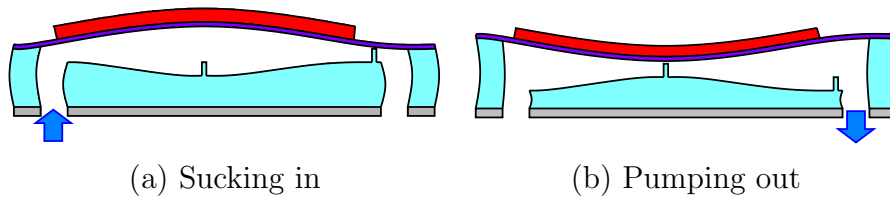

(a) Sucking in   (b) Pumping out

Figure 3. Schematic of the reciprocal pumping sequence.

control the flow direction, see figures 1 and 2. The single actuator design is achieved by exploiting an area of reversed flexure at the interface between the elastomer and the thin glass diaphragm to which the PZT is bonded. By appropriate positioning of the two throttles along the pump channel it is possible to implement pumping.

Figure 2 shows the basic components of the pump. The micro channel is cast on a polydimethylsiloxane (PDMS) layer bonded onto on a glass substrate. The top surface of the PDMS layer is covered by a glass coverslip, whose reverse face is bonded to a PZT piezoelectric bimorph disk. When an electric voltage is applied to the PZT disk and the device is deformed as shown in figure 3 (a), the channel volume (pump chamber) increases and the working fluid flows into the chamber from the inlet. The polarity of the voltage applied to the PZT disk and the device deformation is inverted, discharging the contained fluid as shown in figure 3 (b). Alternating this reciprocating process results in a net transport of fluid. When the elastomeric substrate is deformed, the clearances between the weirs and the cover glass increase or decrease, thus acting as antiphase throttles which determine the direction of flow. The close-to-open ratios of

the throttle flow resistances ratios (throttle resistance ratios) yield pumping efficiencies. The maximum value of the throttle resistance ratio of a double-depth throttle [4] is about 8:1. The maximum reported flow rate of a pump employing the throttles is 1.15 ml/min and the pump overcomes a back pressure of 40 kPa [11].

In this study we report the enhanced performance of a LMTP, by focusing the strain generated in the elastic substrate to increase displacement amplification within the microstructures in order to achieve increased pump performance. Pump performance depends on the pump stroke and the throttle efficacy, i.e. elastomeric substrate deformation. The top and bottom surface of the elastomeric layer are governed by the glass cover bonded to the PZT actuator and the rigid glass base, respectively. The side walls have free surfaces and the deformation in the horizontal direction is unbounded as in previous MTPs. It is expected that controlling the horizontal strain within the elastomer substrate can be employed to optimise the deformation in the channel region and thus enhance the pump performance.

In order to control the strain within the PDMS layer we embed a polymethylmethacrylate (PMMA) annular ring into the elastomeric substrate. The ring is used to restrict the horizontal deformation of the elastomeric substrate and increase the vertical deformation which acts on the channel and throttle walls, thus increasing pump stroke and throttle efficacy. In this study, a fabrication process was developed to manufacture devices with PMMA rings embedded within the elastomer. In order to better understand the effect of the embedded ring on the elastomer deformation finite elemental method simulations were conducted. Finally devices including rings were fabricated and their throttle efficacy and pumping flow rate were experimentally measured.

2. Pump Specifications

The microthrottle pumps developed in this study have a similar basic construction to those previously reported [4, 5, 6, 7]. The dimensions of the PDMS substrate layer were 18 mm square with a thickness of 1.5 mm, see figure 1. The microstructured channels were 14 mm long, 100 μm deep and 1.0 mm wide and both ends are connected to cylindrical through vias which were punched into the substrate. The throttle length (in the direction of flow) is 100 μm and the throttle surfaces are recessed by 15 μm. The central inlet throttle is offset from the centre by 1 mm in the direction to the inlet. The outlet throttle is located 7.5 mm downstream from the centre throttle. The PDMS was bonded onto a 1.2 mm thick glass base and an 18mm square, 110 μm thick, coverglass, whose upper face was coated with circa 250 nm of chrome by evaporation to provide for electrical connection to the lower PZT, was bonded onto the PDMS top surface. The 12.7 mm diameter piezoelectric actuator disk was then aligned such that its centre sits directly over the inlet throttle and was bonded to the top of the coverglass with conductive epoxy adhesive. In order to estimate the throttle efficacy, we also made single throttle devices which contained a single centrally positioned throttle.
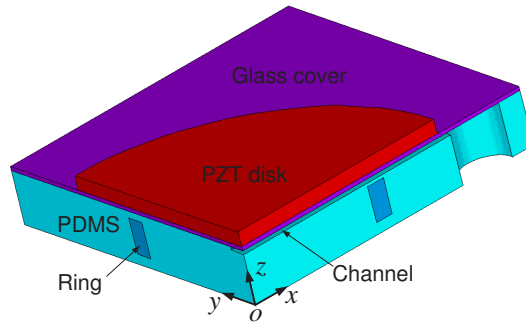
Figure 4. Quarter model for FEM analysis.

In the case of the novel PDMS/PMMA composite devices, the elastomeric substrate contains an additional PMMA ring. Here, the 'ring diameter' is defined as the mean value of the inner diameter and outer diameters. Previously reported [4] vibrometric measurements of the deflection of an operational MTP obtained using a Polytec PSV400-series scanning laser vibrometer (Lambda Photometrics Ltd, Harpenden, UK) displayed that the composite MTP structure undergoes a series of complex compressive and tensile stresses below the upper face (that is to say in the microstructure region). These stresses result in a circular annulus which acts as a mechanical node having a diameter of 8.5 mm. If the embedded PMMA ring is not matched to the diameter of this node, stresses would be generated between the cover glass and the ring and the dynamic motions of the elastomer would be restricted when the operating the pump at high frequencies. Therefore, it was proposed that the most suitable ring diameter for inclusion within the PDMS substrate was 8.5 mm.

The ring thickness in the radius direction is 1.0 mm. The ring is vertically positioned 300 μm from the bottom of the elastomer layer and its height is 1.0 mm: the distance between the top of the ring and the bottom of the microchannel is 100 μm. The ring is positioned concentrically with the centre of the PZT disk.

3. Finite element method analysis of the effect of a ring on the elastomeric substrate layer deformation

3.1. Simulation conditions

In order to better understand the effect of a PMMA ring on the PDMS elastomer deformation finite element method analysis was conducted. A 28,000 node mesh defining 18,000 elements was developed with ANSYS ver. 10.0. In operation the elastomer layer of the micropump is dynamically deformed; the analysis of its dynamic process is extremely complex. Here, the analysis is limited to static deformation of a simple model shown in figure 4. For simplicity the model examines the deformation caused to a rectangular straight flow channel. The design is symmetric about two axes and therefore we model one quarter of its geometry. A coverglass covers the top of PDMS and a PZT disk is
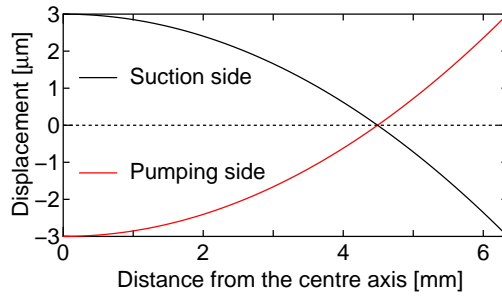
Figure 5. Given condition of the PZT disk deformation.

Table 1. Properties of the materials.

	PDMS	PMMA	Glass	PZT
Elastic modulus [GPa]	0.001	3.2	73	52
Poisson's ratio	0.4999	0.35	0.30	0.31

positioned at the top centre of the glass. A PMMA ring, with ring diameter of 8.5 mm, is included in the PDMS layer and is concentric with the PZT disk. All components are completely bonded to each other. The dimensions of the components accord with the experimental devices. The material properties described in table 1 are identical to those used for FEM modelling in our previous papers [4, 5, 6]. A Cartesian coordinate system is defined such that x, y and z represent the directions of flow, span and thickness, respectively. The origin is located at the centre of the bottom surface of the PDMS layer because the bottom surface is assumed to be stationary whilst the top surface is deformed by the PZT disk.

The deformation of the PZT disk/glass coverslip composite is achieved by applying a potential difference, which in this study is 180 V. Previous experimental measurements of the displacements at the centre and the edge of the PZT disk were ± 3 μm and ∓ 3 μm, respectively [6]. The PZT deformation is axially symmetric and, approximating the experimental results obtained the previous study, it is assumed that the deformation along the line of the diameter is parabolic, as shown in figure 5.

3.2. Simulation results

The deformations predicted for both the standard LMTP and one with an embedded PMMA ring in suction stroke are shown in figure 6. The colour contour indicates the displacement in z-direction. Note that the deformation is bombastically depicted for easy observation. These results demonstrate that inclusion of the ring amplifies the downward displacement of the bottom of the flow channel within the radius of the ring and amplifies the upward displacement of the bottom of the flow channel outside the radius of the ring.
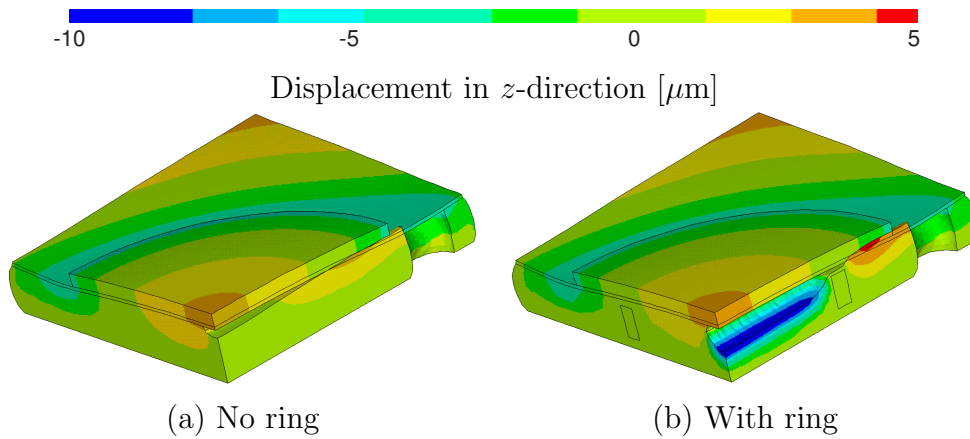
(a) No ring   (b) With ring

Figure 6. Deformed device aspects and contours of z-direction displacement in suction stroke.

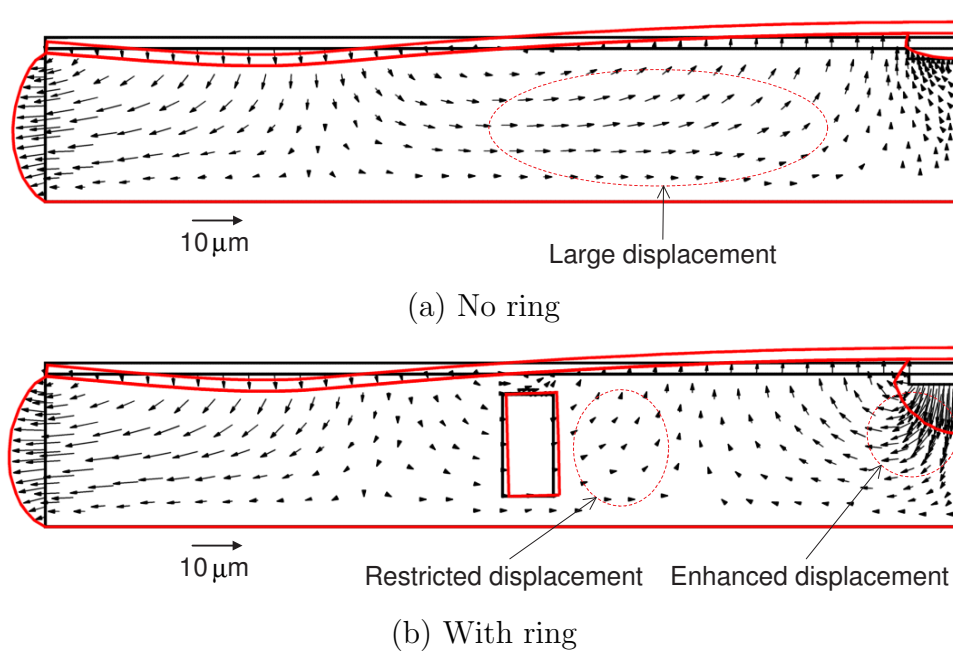(a) No ring

(b) With ring

Figure 7. Deformed device aspects and contours of the displacement vectors in y-z cross-sectional area in suction stroke.

Figure 7 shows the contours of the displacement vectors in the y-z cross-section at $x = 0$ within the deformed PDMS substrate. The black lines indicate the resting positions and the red lines indicate the final static deformed positions. The deformation is again bombastically depicted in this figure. The arrows display the direction and magnitude of the displacement at each location. During the suction stroke, the inner area of the PZT disk pulls up the coverglass and PDMS. As the Poisson's ratio of PDMS is approximately 0.5 (i.e. the total volume of the PDMS layer does not vary when it deforms elastically) the volume of the elastomer pulled up by the PZT disk is filled by displacement of elastomer in close proximity. Whilst useful effects are observed in the
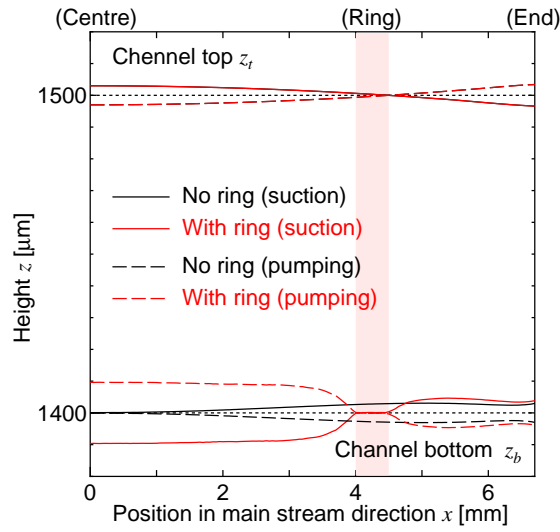
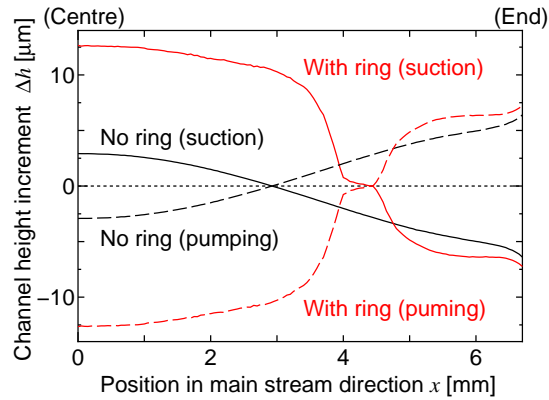**Figure 8.** Comparison of the displacements of the channel top height z_t and the channel bottom height z_b.

Figure 9. Comparison of the increment Δh of the channel height h. The channel height h is given by the difference between the channel top height z_t and the channel bottom height z_b.

case of the standard LMTP [4, 5, 6], the environmental bulk region moves toward the centre and this displacement limits the total volume increase of the flow channel. The deformation effect of the PZT disk is wasted and the channel deformation is small. In comparison, in the LMTP with the embedded PMMA ring, the displacement of the environmental bulk region is restricted by the ring. This causes the region around the channel to be displaced in order to cancel the volume increase due to the PZT disk motion. The result is that the channel deformation is amplified and hence its volume is increased.

In order to estimate the effect of the ring quantitatively, the displacements of the top and bottom of the channel along the centre line in the y-direction are depicted in figure 8. Figure 9 shows the increments Δh of the channel heights h (i.e. the gap between the top

and bottom) along the centre line in the y-direction. In the case of the standard LMTP (no ring), the channel bottom around the centre ($x = 0$) is only slightly raised. The increment of the chamber volume for fluid suction is predominantly provided by only the displacement of the glass cover slip. In the case of the LMTP with an embedded PMMA ring, the displacement of the channel bottoms are amplified within the circumference of the ring and the flow channel volume is significantly increased. Similarly the ring also enhances raising of the channel bottoms outside the circumference of the ring. Therefore, the addition of the ring increases the pump ability to suck in a greater volume of fluid during each pumping stroke.

Examining the pumping stroke it can be seen that each displacement is in the opposite direction to that in the suction stroke and the characteristics of the deformation are similar to those observed in the suction stroke. The chamber volume reduction is enhanced by the ring and the outlet gap is amplified. Therefore, inclusion of the ring should prove equally effective at enhancing the pumping stroke.

In a LMTP, throttles are situated at the centre and the end of the channel. The simulation results indicate that inclusion of the ring enhances the channel displacement during the suction and pumping strokes and indicates that greater opening and closing displacements of the throttles is also obtained, i.e. the throttle resistance ratios are increased. This suggests that the inclusion of a ring should provide both increased pump stroke volume and increased flow control.

To summarise, it is predicted that a PMMA ring embedded into the PDMS substrate will provide control over the PDMS deformation enhancing both chamber volume variation and throttle resistance ratios.

4. Fabrication and assembly process

LMTP fabrication has been previously reported [4, 5, 6]. The new devices incorporating rings were made almost identically, with the exception of the process used to fabricate the PDMS layer with the embedded PMMA ring. This fabrication process is briefly summarized.

PDMS substrates were cast using double depth molds, which were fabricated on three inch silicon wafers from two layers of epoxy negative photoresist 'SU-8'. First, the thin 15 μm thick SU-8 layer was spun, pre-exposure baked and patterned by UV exposure through a photomask using a Suss MJB3 contact aligner. The wafer was then post-exposure baked and rinsed. The 100 μm thick SU-8 layer was spun on top of the first layer. The second photomask was aligned to the first layer and exposed. The wafer was then post-exposure baked and developed leaving the SU-8 mold on the silicon wafer.

The PDMS microstructured substrates were cast from the molds using Dow Corning Sylgard 184 PDMS and the PMMA rings. The subsequent assembly is illustrated. The PMMA rings were fabricated by conventional CNC machining. A 300 μm thickness PDMS base sheet was cast on a flat plate in the standard way (figure 10 (a)). The PMMA ring was precisely positioned on top of the PDMS sheet. The natural 'stickiness'
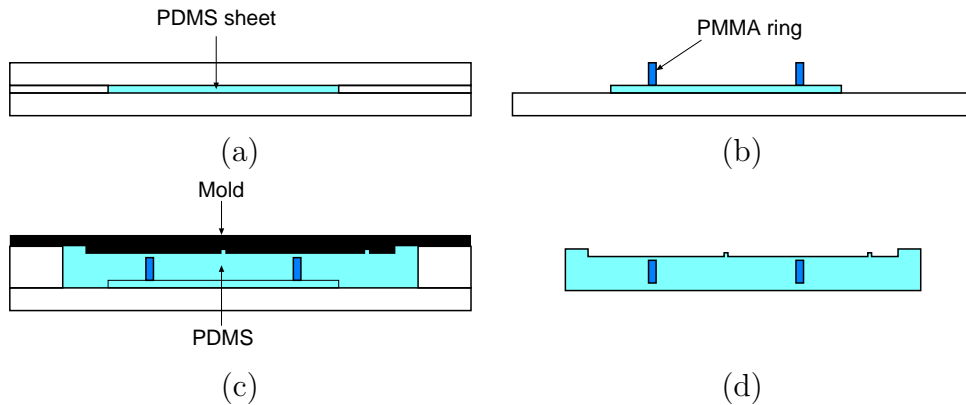
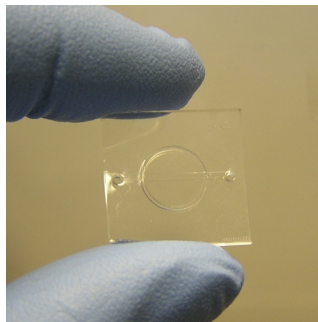**Figure 10.** Process to cast a PDMS substrate including a PMMA ring.

Figure 11. Image of a polymerised PDMS substrate including a PMMA ring.

of the cured PDMS sheet was sufficient to immobilise the PMMA ring during the casting process (figure 10 (b)). The remaining part of the PDMS substrate was cast with the double depth channel mold (figure 10 (c)). Our normal process is to bake the PDMS at 90 °C for 2 hours; however, it was found that if a PDMS substrate which incorporates a PMMA ring is baked in the same manner, large strain develops in the substrate due to a small amount of shrinkage which normally occurs as the PDMS cures. To overcome this effect the PDMS substrate including the PMMA ring were polymerised at room temperature for 2 days. To ensure full polymerisation the composite was then baked at 60 °C for 4 hours. The long low temperature curing process also resulted in the two PDMS layers becoming permanently bonded together and encasing the PMMA ring (figure 10 (d)). The PMMA rings curved out by CNC machining had slightly rough surfaces. PDMS was penetrated into the roughness of the surfaces and the attachment between the PDMS and PMMA was made stronger than that in the case of smooth surfaces. An image of the cast PDMS structure including a PMMA ring is shown in figure 11.

The remaining assembly process is identical to that of our previously reported MTPs [4, 5, 6]. The PDMS was bonded onto a glass microscope slide which was diamond drilled to match the two connection vias. A coverglass whose upper face was coated with chrome by evaporation was then bonded onto the PDMS top surface. The piezoelectric actuator

disk was then aligned and bonded to the top of the coverglass with conductive epoxy adhesive. Finally 1.6 mm od 0.5mm id PEEK inlet and outlet tubes were secured with epoxy adhesive.

5. Experiments

Because micro throttles do not completely close, their resistance ratios strongly affect the performances of the MTPs in which they are employed. In order to evaluate the effect of incorporating a PMMA ring into the PDMS substrate on the throttle resistance ratio, devices which have single throttles at the centre of their flow channels were fabricated. These throttles were characterized by mass transfer to a Sartorious 210s precision microbalance at a series of precise pneumatically controlled pressures P between 1 kPa and 40 kPa with applied D.C. voltages of ± 180 V and the flow rate Q was measured. The flow resistance of the device R is defined as $R \equiv P/Q$ and suffixes, 'open' and 'close', represents the throttle is opened and closed, respectively. Throttle resistance ratio is defined as R_{close}/R_{open} and illustrates the throttle efficacy quantitatively.

Throttle performance is intimately related to the external flow resistances of tubing in the associated measuring system. In order to assess the test throttle objectively the resistances of the tubing were measured and allowed for.

MTPs were tested by alternately applying $+180$ V or -180 V and varying the frequency f, which is up to 2000 Hz because higher frequency results in loosing the pumping rate [5]. Waveform generation was via a bespoke microcontroller system and 'H-bridge' drive electronics employing power-FETs. The microcontroller allowed predetermined sequences of frequency steps to be applied in order to characterize frequency-dependent behaviour. As we have reported [6], the possibility of bubble formation is prevented by mildly restricting the drive waveform rise and fall times by using a simple series resistor to form a 200 μs time constant with the PZT capacitance. The drive-frequency/forward-pumping rate relationship with zero back pressure was obtained by running the pump under microcontroller control. Microbalance data were processed in real time by software written in Labview® (National Instruments) to obtain mass flow rate values for each drive frequency f. The relationship between flow rate Q and back pressure P was then measured at the frequency f which previously resulted in the highest flow rate with zero back pressure.

In order to confirm that the suitable ring diameter is 8.5 mm as described in section 2, three LMTPs incorporating 7.5, 8.5 and 9.5 mm diameter embedded rings were fabricated and tested.

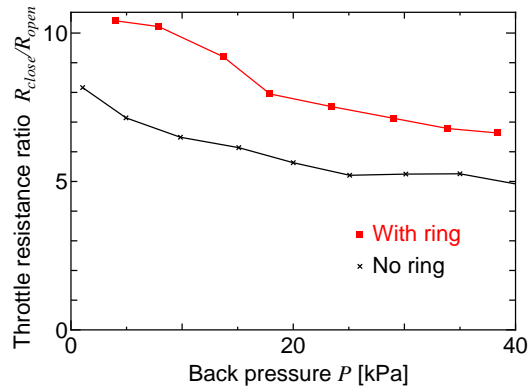In all cases de-ionised water was used as the working fluid.

Figure 12. Relation between the throttle resistance ratio R_{close}/R_{open} and the applied back pressure P.

6. Results and discussion

As described in section 3.2 the FEM results indicate that an embedded ring increases the open and closed throttle positions. In order to experimentally verify the effect on throttle deformation the throttle resistance ratios R_{close}/R_{open} of single throttle devices which were fabricated without a ring and with a ring are compared, see figure 12. The resistance ratio of the device including the ring is approximately 40 % greater at low pressure and 30 % greater at high pressure than that of the device without a ring. These results demonstrate that the inclusion of the ring does enhance the throttle resistance ratio under static deformation conditions.

The pumping rates Q generated by the LMTPs driving under zero pressure condition ($P = 0$) are displayed as a function of frequency f in figure 13. All pumps displayed similar behaviour to previously reported pumps [5] having both low and high frequency peaks. However the higher frequencies at which the pumps flow rates peak vary by approximately 500 Hz. It is probable that the new LMTPs, with embedded PMMA rings, have differing dynamic resonances in their composite structures which result in variations in the pumping rates as a function of drive frequency f. Comparing the LMTPs with embedded rings it can be seen that the device with the suitable diameter ring significantly out performs the devices with either the small or large rings. This is in accord with the predictions of section 2, i.e. that the larger or smaller rings might restrict the PZT disk and cover glass motion. The LMTP with the 8.5 mm diameter ring achieves pumping rates almost double those of the other LMTPs, with either the 7.5 mm, 9.5 mm rings or the standard LMTP, over the entire frequency range. This means that the suitable ring mainly affects on the static deformation of the device and establishes the reasonability of the FEM simulation limited to static deformation. The maximum pumping rate of 2.2 ml/min was achieved at 1500 Hz.

Pumping rate Q as a function of back pressure P was examined at the peak pumping frequency (1500 Hz and 1800 Hz respectively) for both the LMTP with the 8.5 mm
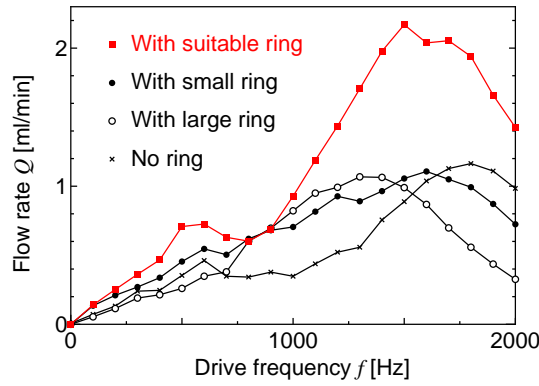
Figure 13. Comparison of the flow rate with the ring diameter. The diameters of the suitable, small and large rings are 8.5, 7.5 and 9.5 mm, respectively
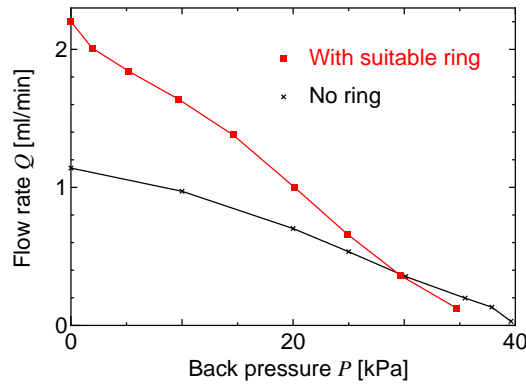

Figure 14. Relation between the flow rate and the applied back pressure.

diameter ring and the standard LMTP, see figure 14. Whilst both pumps are able to achieve similar maximum pressure performance the LMTP with the 8.5 mm diameter ring has the higher pumping rate at all pressures up to 30 kPa.

7. Conclusion

We have demonstrated that interesting forms of dynamic microstructures are possible with elastomeric substrates which are not possible using rigid substrates. We have developed a technique for fabricating composite polymeric PDMS/PMMA microstructures which focus the internal strains generated during static and dynamic deformations. This focusing is employed in order to enhance the displacement amplification effects in the elastomeric microstructures to significantly improve throttle resistance ratios and pumping performance of linear micro throttle pumps (LMTPs).

We demonstrate a LMTP which was a PMMA ring embedded into the PDMS layer. The optimal ring diameter (8.5 mm) is identified as that which best matches the mechanical node of the PZT disk actuator/glass composite.

The enhanced throttle device achieved throttle resistance ratios 1.4 times greater

than those of the standard microthrottle design. The enhanced LMTP achieved a peak pumping rate of 2.2 ml/min and a working back pressure of 34 kPa.

We can crudely assign a figure of merit to such pumps by means of a maximum pump-rate [ml/min] × maximum backpressure [kPa] product. This LMTP design yields a figure of merit of 75 Pa·l/min whereas our previous LMTP design [5] yielded a figure of 44 Pa·l/min.

The enhanced LMTP, by further utilising the elastomeric nature of PDMS substrates, has extended the performance of MTP-type micropumps: by delivering fluid transport rates beyond two millilitres per minute, whilst offering worthwhile backpressures and solid-phase suspension compatibility, within a compact, simple, straightforwardly fabricated structure.

References

[1] Laser D J and Santiago J G 2004 A review of micropumps *J. Micromech. Microeng.* **14** R35–R64

[2] Woias P 2005 Micropumps - past, progress and future prospects *Sensors Actuators* B **105** 28–38

[3] Weigl B, Domingo G, LaBarre P and Gerlach J 2008 Towards non- and minimally instrumented, microfluidics-based diagnostic devices *Lab Chip* **8** 1999–2014

[4] Johnston I D, Tracey M C, Davis J B and Tan C K L 2005 Micro throttle pump employing displacement amplification in an elastomeric substrate *J. Micromech. Microeng.* **15** 1831–1839

[5] Tracey M C, Johnston I D, Davis J B and Tan C K L 2006 Dual independent displacement-amplified micropumps with a single actuator *J. Micromech. Microeng.* **16** 1444–1452

[6] Johnston I D, Tracey M C, Davis J B and Tan C K L 2005 Microfluidic solid phase suspension transport with an elastomer-based, single piezo-actuator, micro throttle pump *Lab Chip* **5** 318–325

[7] Johnston I D, Davis J B, Richter R, Herbert G I and Tracey M C 2004 Elastomer-glass micropump employing active throttles *Analyst* **129** 829–834

[8] Fujiwara T, Ohue H, Ushijima T and Kitoh O 2007 Optimization of Channel Geometry and Pumping Conditions for an Alternate Pumping Microreactor *J. Fluid Sci. Technol.* **2** 389–399

[9] Lee Y, Shih C, Tabeling P and Ho C 2007 Experimental study and nonlinear dynamic analysis of time-periodic micro chaotic mixers *J. Fluid Mech.* **575** 425–448

[10] Tan C K L, Tracey M C, Davis J B and Johnston I D 2005 Time-interleaved micromixier with elastmeric valves *J. Micromech. Microeng.* **15** 1885–1893

[11] Tracey M C, Johnston I D, Davis J B and Tan C K L 2006 Suspension-Compatible Elastomer-Glass Micropumps Employing Linear Topology *Proc. IET Seminar on MEMS Sensors and Actuators* 31–38